

## Supplementary Material (SI)

### Three-Dimensional Auxetic Properties in Group V-VI

#### Binary Monolayer Crystals $X_3M_2$ ( $X=S, Se, M=N, P, As$ )

Yan Chen<sup>1</sup>, Xiangbiao Liao<sup>4</sup>, Xiaoyang Shi<sup>4</sup>, Hang Xiao<sup>2,4,\*</sup>, Yilun Liu<sup>3,\*</sup> and Xi Chen<sup>2,4</sup>

<sup>1</sup> International Center for Applied Mechanics, State Key Laboratory for Strength and Vibration of Mechanical Structures, School of Aerospace, Xi'an Jiaotong University, Xi'an 710049, China

<sup>2</sup> School of Chemical Engineering, Northwest University, Xi'an 710069, China

<sup>3</sup> State Key Laboratory for Strength and Vibration of Mechanical Structures, School of Aerospace, Xi'an Jiaotong University, Xi'an 710049, China

<sup>4</sup> Center for Advanced Materials for Energy and Environment, Department of Earth and Environmental Engineering, Columbia University, New York, NY 10027, USA

\* E-mail: (Y.L.) [yilunliu@mail.xjtu.edu.cn](mailto:yilunliu@mail.xjtu.edu.cn); (H.X.) [hx2152@columbia.edu](mailto:hx2152@columbia.edu)

#### Out-of-Plane NPR of 2-D $X_3M_2$

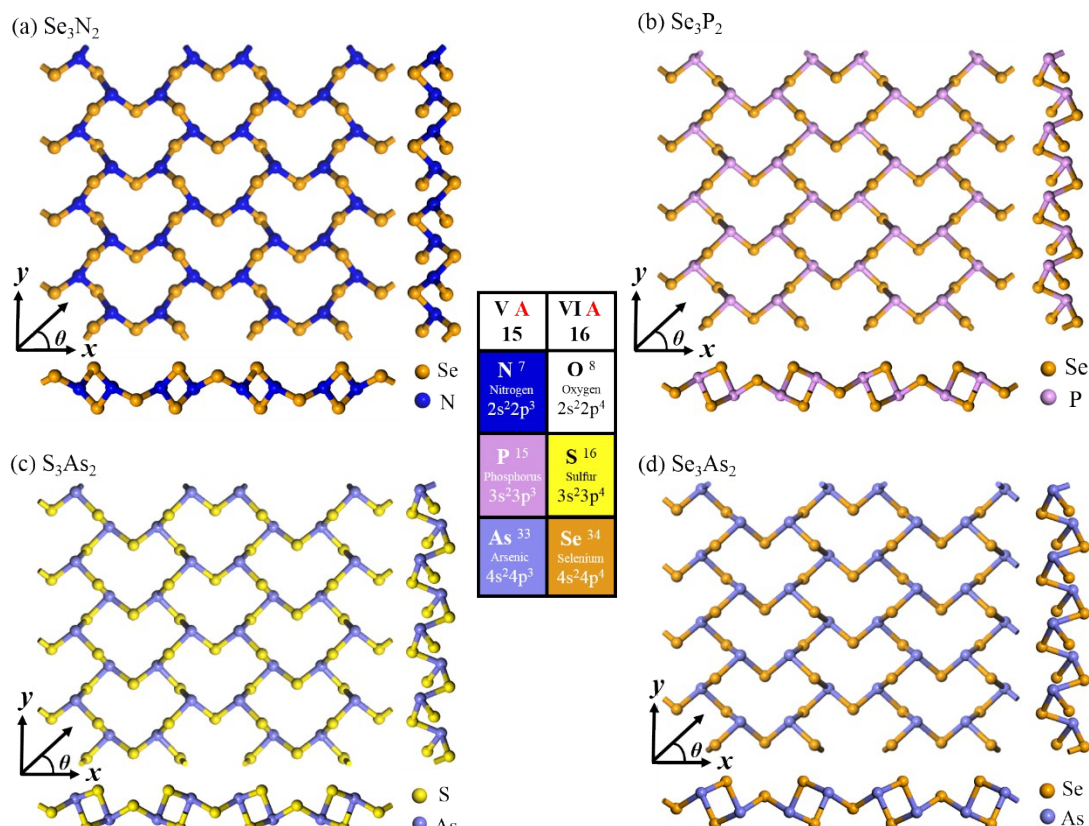


Figure S1 Atomic model of (a)  $Se_3N_2$  (b)  $Se_3P_2$  (c)  $S_3As_2$  and (d)  $Se_3As_2$ . The inset shows group V and VI elements considered in this study (colored).  $\theta$  defines the orientation relative to  $x$  axis.

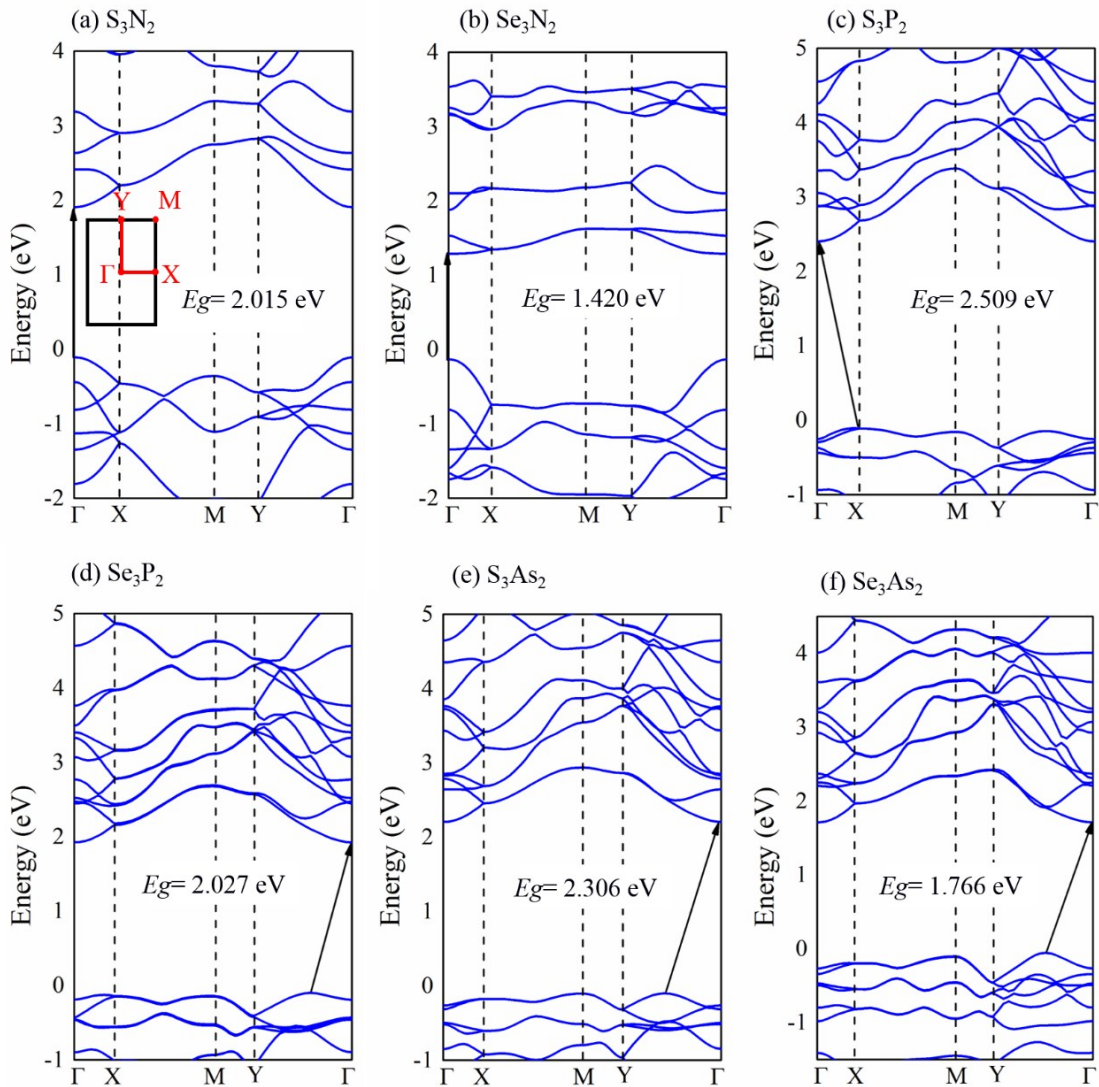


Figure S2 Energy band structures of  $X_3M_2$  ( $X=S, Se$ ;  $M=N, P, As$ ). The inset in (a) shows the Brillouin zone and relevant high-symmetry k-points for all of the 2-D crystals  $X_3M_2$ .

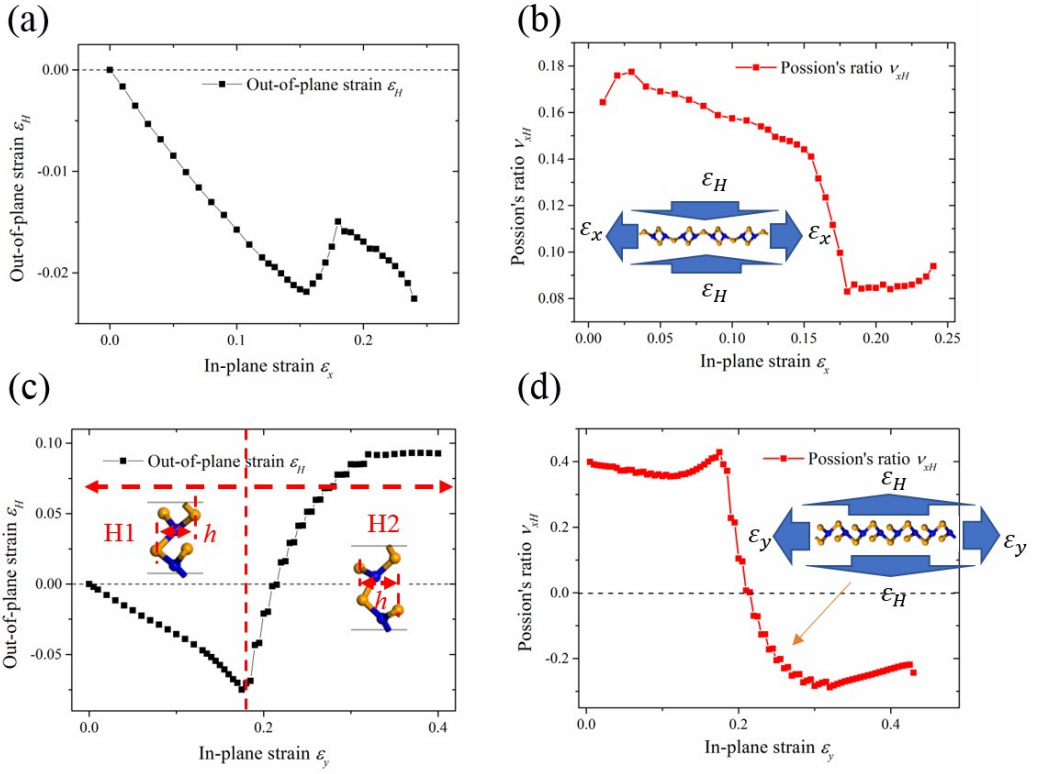


Figure S3 Out-of-plane strain and its corresponding Poisson's ratio of  $\text{Se}_3\text{N}_2$  under tension in  $x$  direction (a), (b) and  $y$  direction (c), (d).

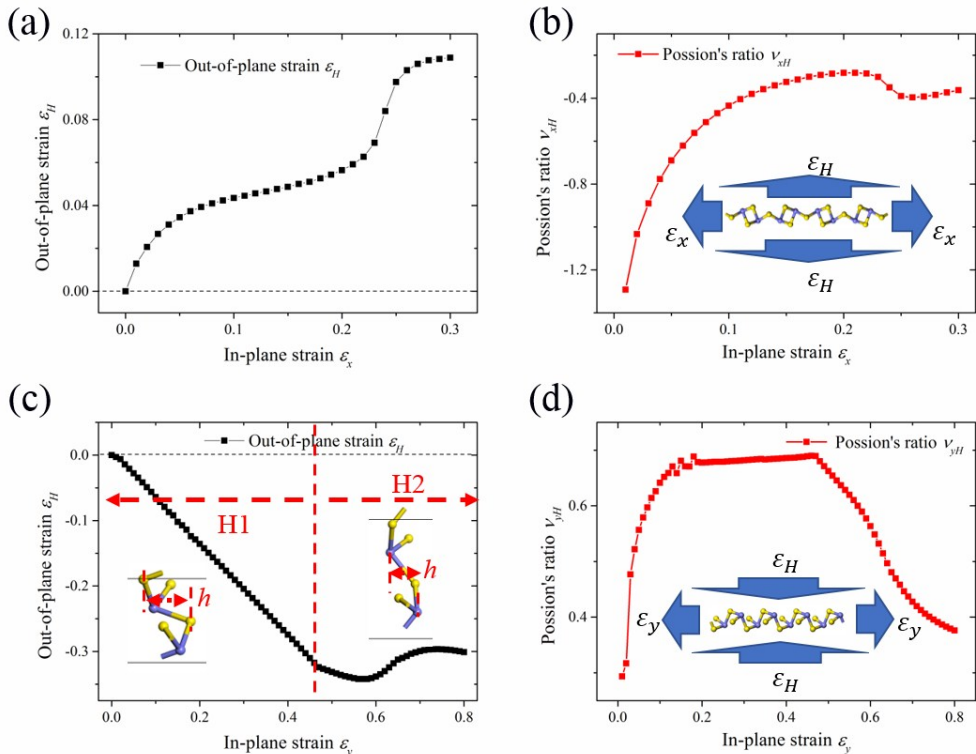


Figure S4 Out-of-plane strain and its corresponding Poisson's ratio of  $\text{S}_3\text{As}_2$  under tension in  $x$  direction (a), (b) and  $y$  direction (c), (d).

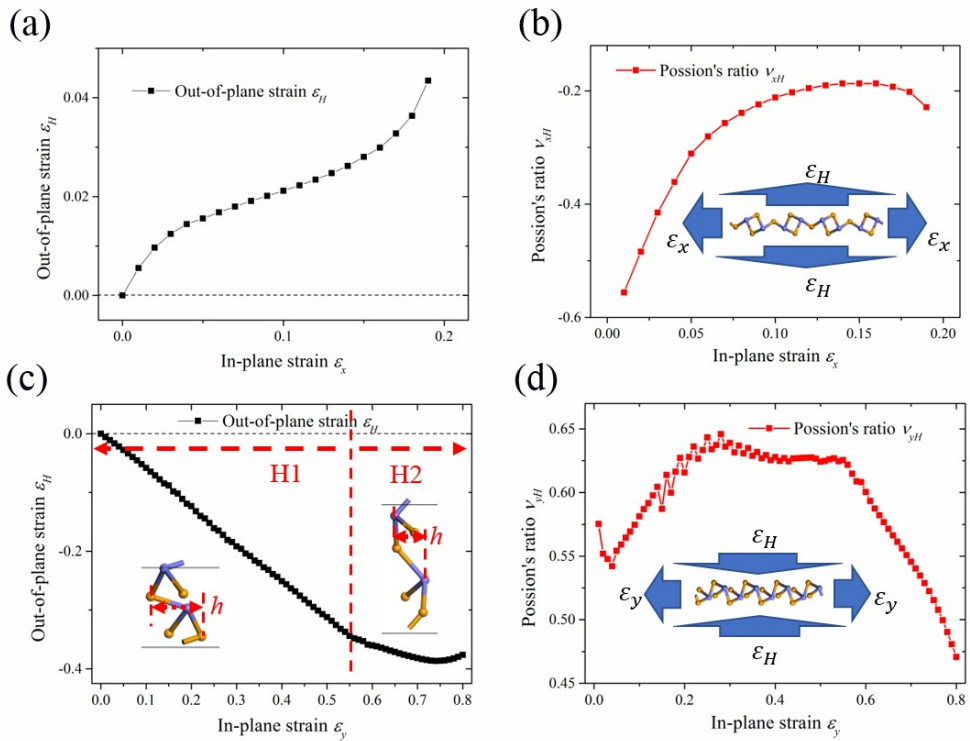


Figure S5 Out-of-plane strain and its corresponding Poisson's ratio of  $\text{Se}_3\text{As}_2$  under tension in  $x$  direction (a), (b) and  $y$  direction (c), (d).

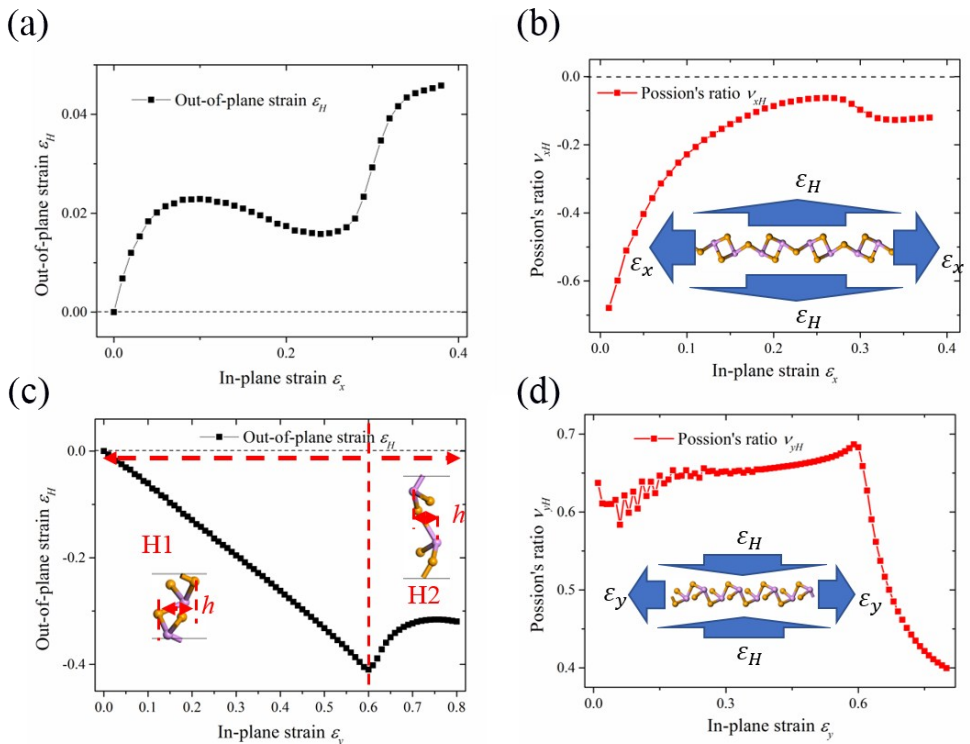


Figure S6 Out-of-plane strain and its corresponding Poisson's ratio of  $\text{P}_2\text{Se}_3$  under tension in  $x$  direction (a), (b) and  $y$  direction (c), (d).

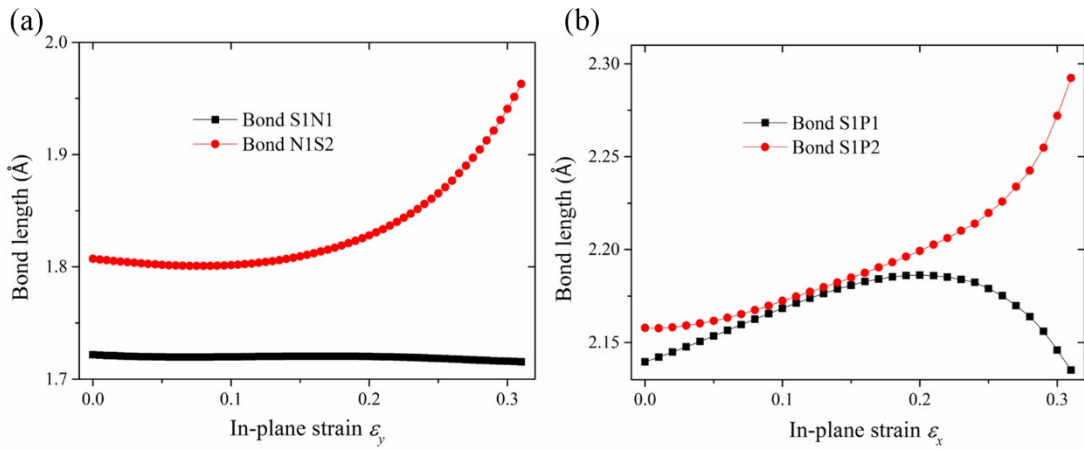


Figure S7 Bond length changes under tension (a) in  $y$  direction for  $\text{S}_3\text{N}_2$  and (b) in  $x$  direction for  $\text{S}_3\text{P}_2$ .

### Cross-Plane NPR of 3-D Bulk Form $\text{X}_3\text{M}_2$

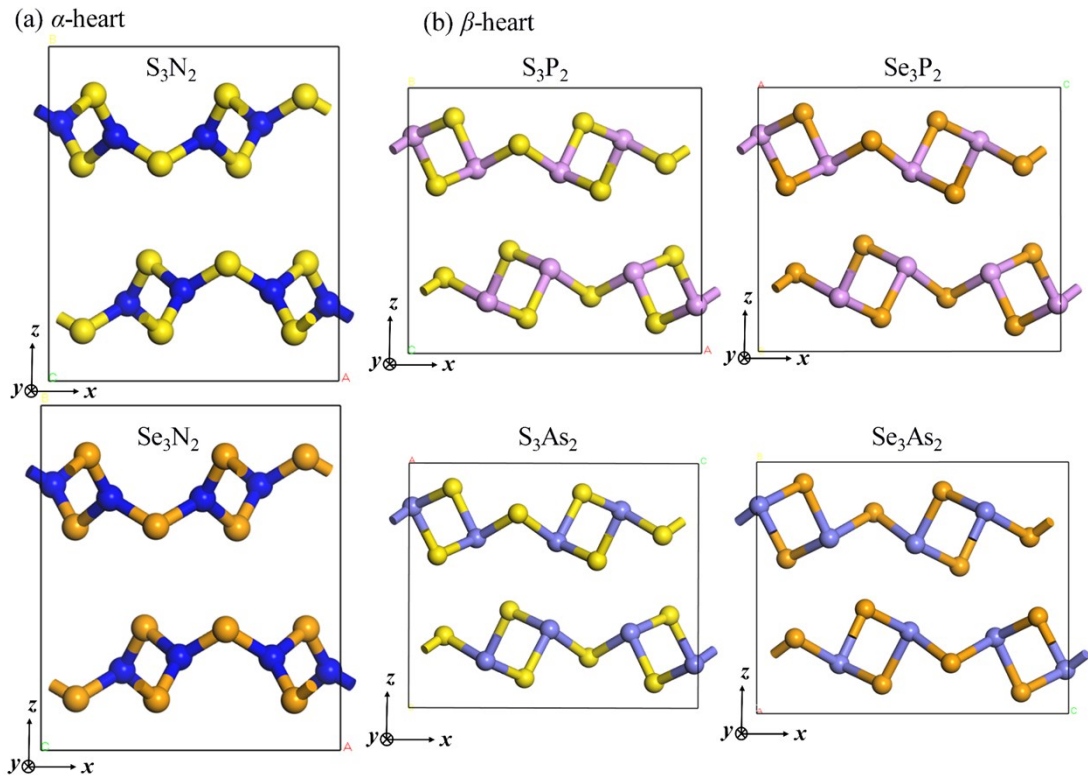


Figure S8 Atomic model of the most energetically favorable stacked (a)  $\alpha$ -heart and (b)  $\beta$ -heart  $\text{X}_3\text{M}_2$  bulk crystal.

Table S1 Cross-plane interlayer Poisson's ratio for  $X_3M_2$  bulk crystals ( $X=S, Se$ ;  $M=N, P, As$ ) and other bulk crystals reported before.

	$\nu_{xH*}$	$\nu_{yH}$
Black phosphorus <sup>1</sup>	~ -0.5	~ 0.3
Bulk arsenene <sup>2</sup>	/	-0.125
Bulk $S_3N_2$	0.325	0.049
Bulk $Se_3N_2$	0.943	0.041
Bulk $S_3P_2$	0.411	<b>-0.457</b>
Bulk $Se_3P_2$	0.192	<b>-0.101</b>
Bulk $S_3As_2$	0.278	<b>-0.025</b>
Bulk $Se_3As_2$	0.152	<b>-0.065</b>

\*

For

black phosphorene and arsenene, x and y represent armchair and zigzag directions, respectively.

### *a*-heart $X_3M_2$ Bulk Crystals

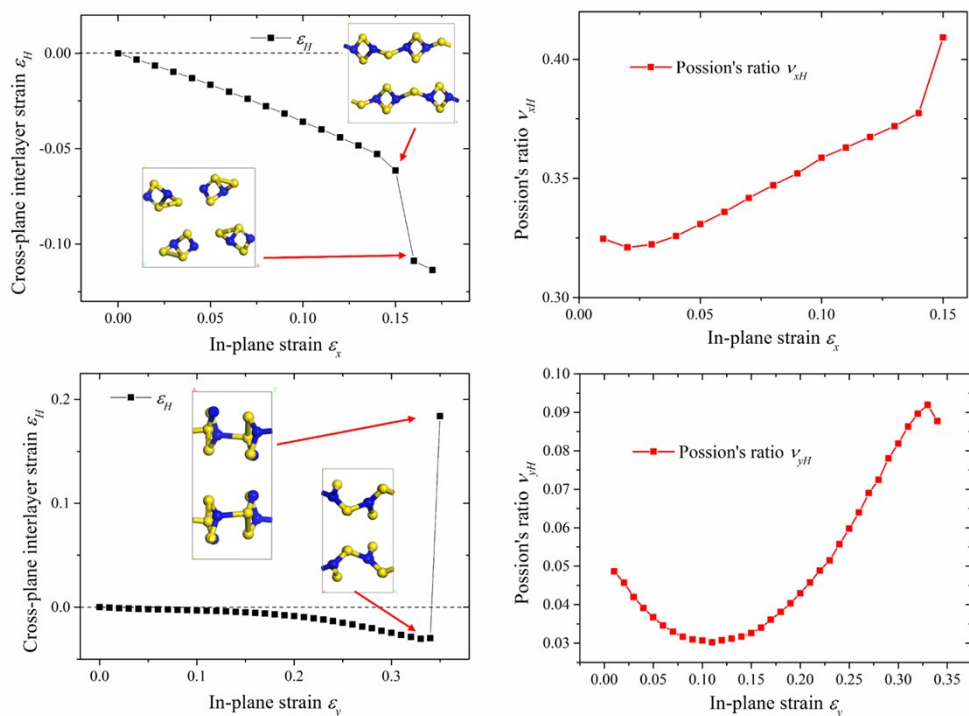


Figure S9 Cross-plane interlayer strain and its corresponding Poisson's ratio of  $S_3N_2$  bulk crystal under tension in x and y direction.

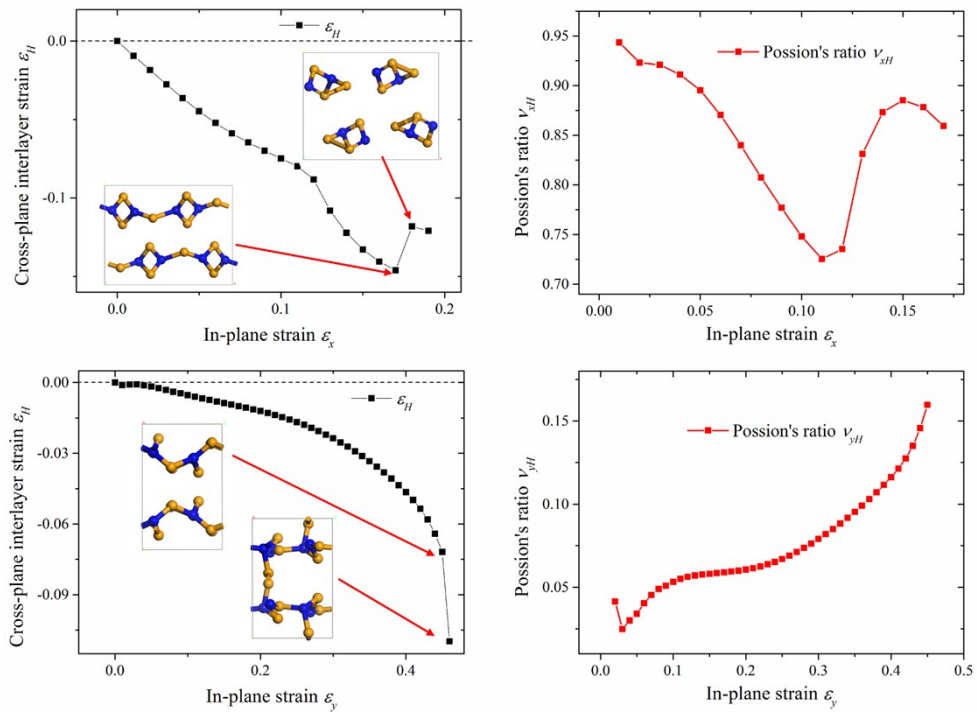


Figure S10 Cross-plane interlayer strain and its corresponding Poisson's ratio of  $\text{Se}_3\text{N}_2$  bulk crystal under tension in  $x$  and  $y$  direction.

### $\beta$ -heart $X_3M_2$ Bulk Crystals

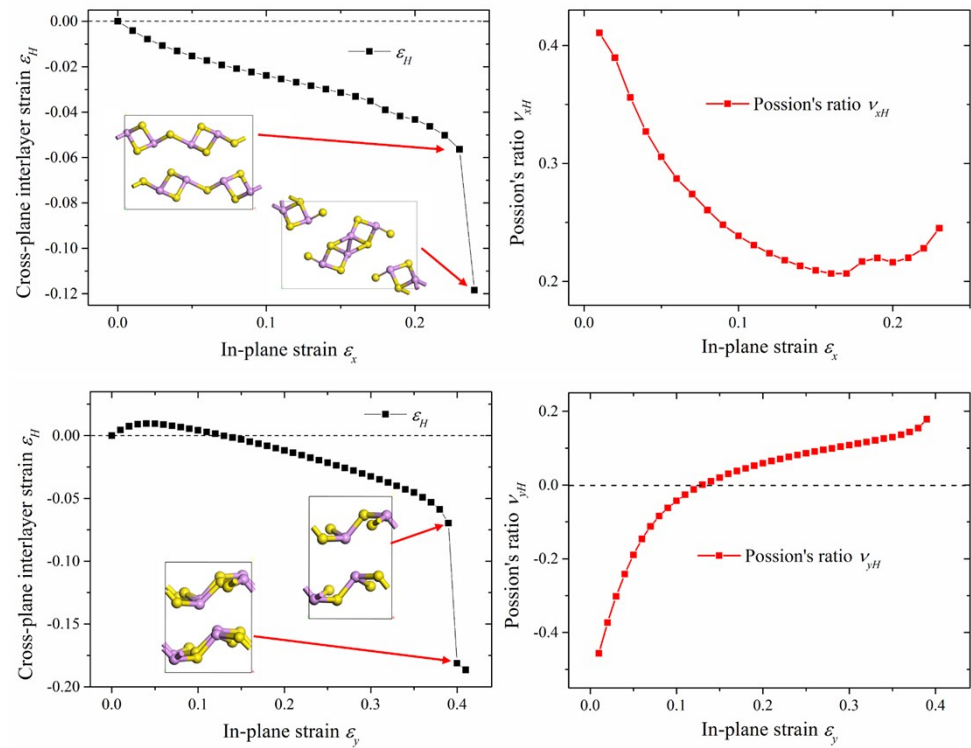


Figure S11 Cross-plane interlayer strain and its corresponding Poisson's ratio of  $\text{S}_3\text{P}_2$  bulk crystal under tension in  $x$  and  $y$  direction.

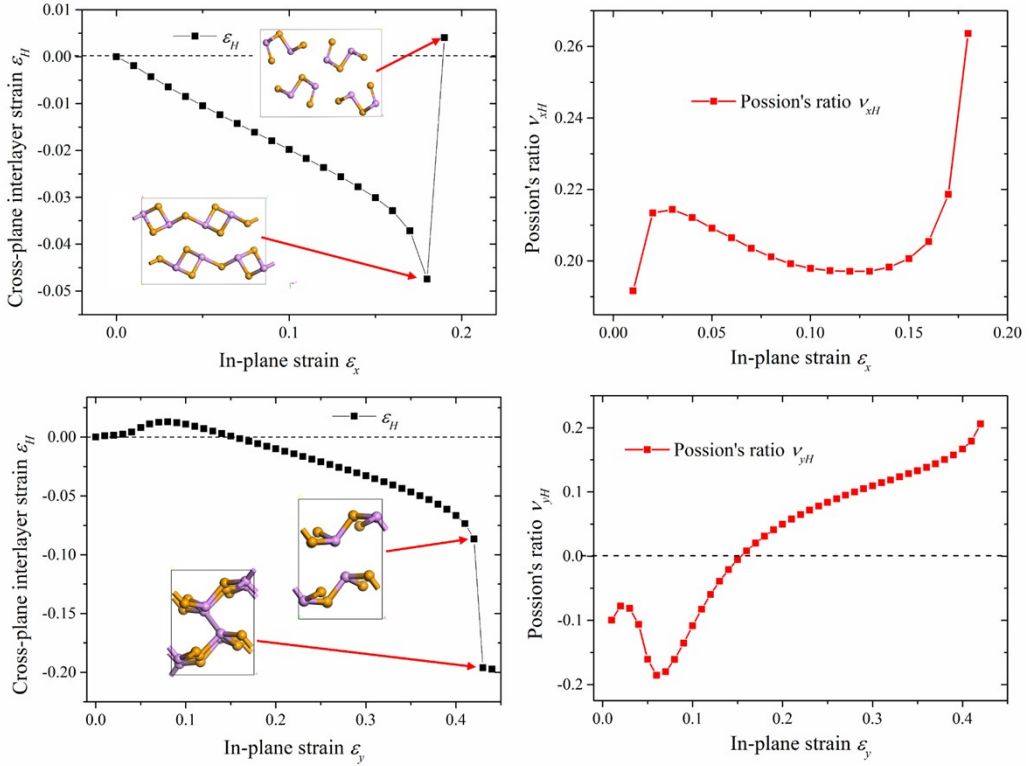


Figure S12 Cross-plane interlayer strain and its corresponding Poisson's ratio of  $\text{Se}_3\text{P}_2$  bulk crystal under tension in  $x$  and  $y$  direction.

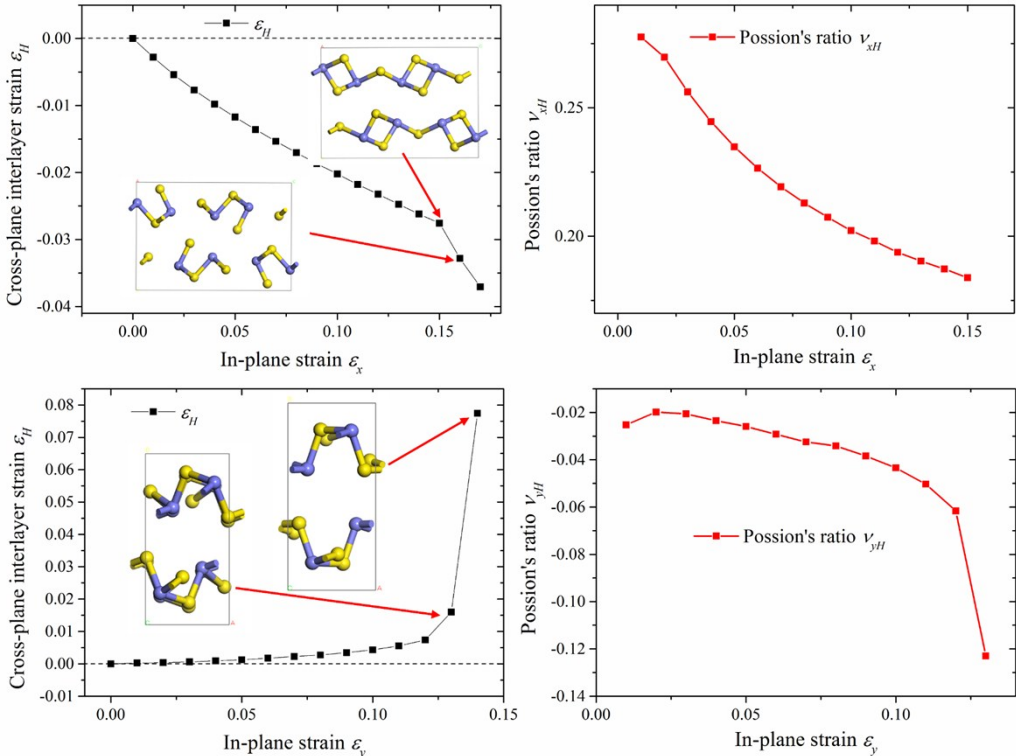


Figure S13 Cross-plane interlayer strain and its corresponding Poisson's ratio of  $\text{S}_3\text{As}_2$  bulk crystal under tension in  $x$  and  $y$  direction.

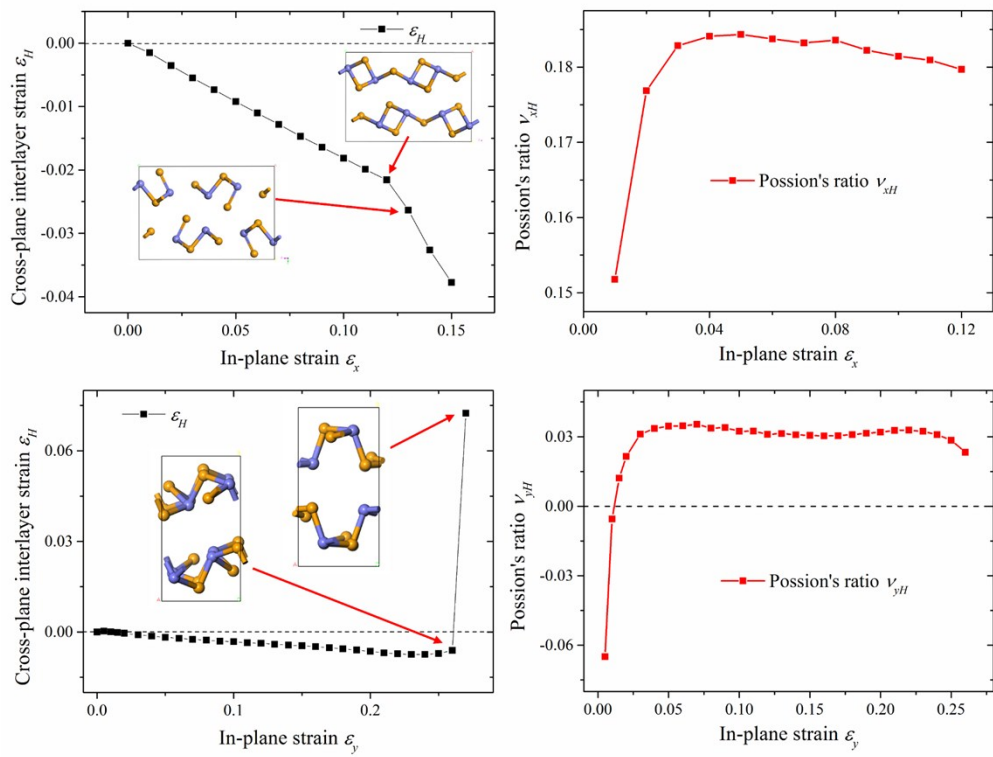


Figure S14 Cross-plane interlayer strain and its corresponding Poisson's ratio of  $\text{Se}_3\text{As}_2$  bulk crystal under tension in  $x$  and  $y$  direction.

## In-Plane NPR of 2-D Crystals $X_3M_2$

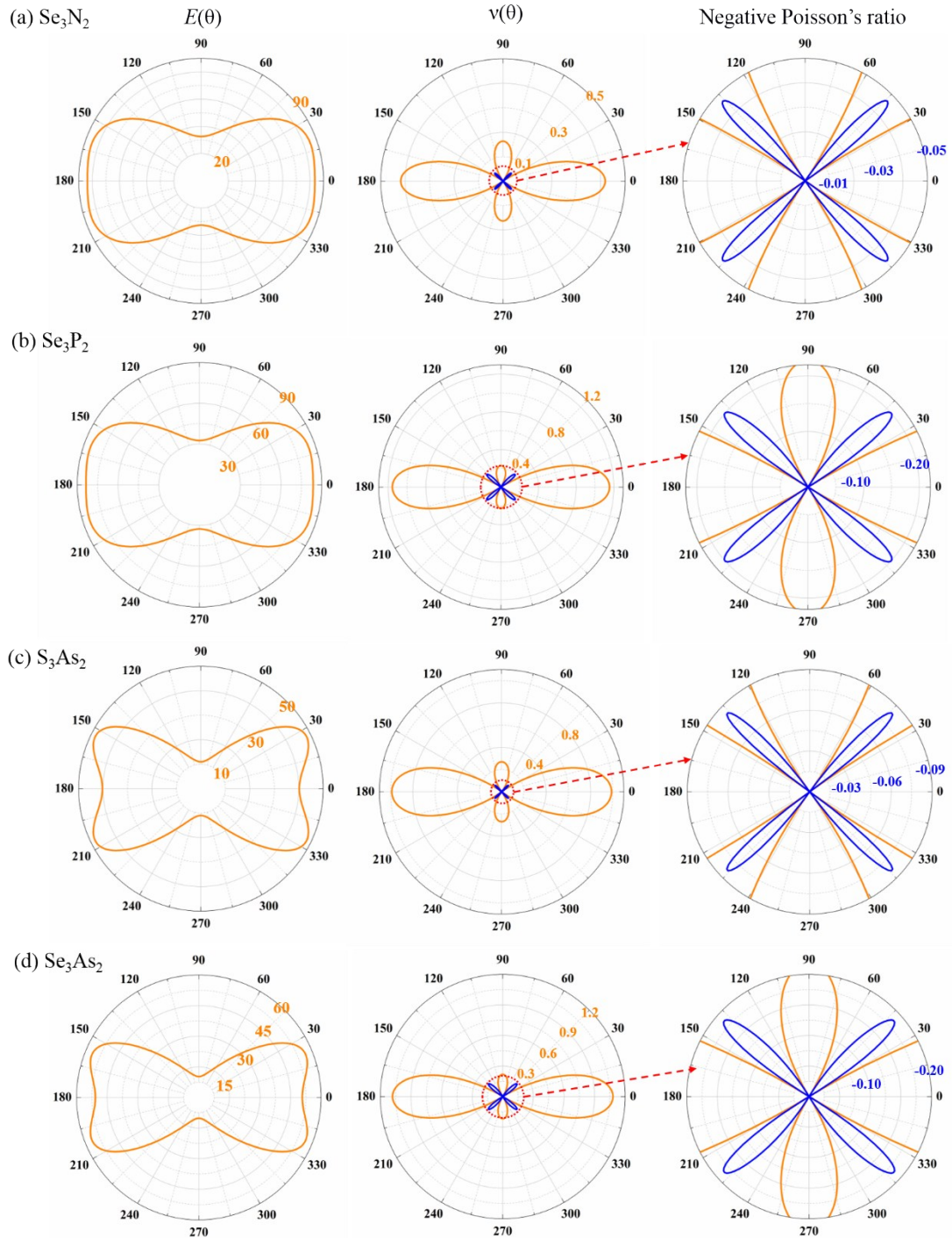


Figure S15. Orientation-dependent in-plane Young's modulus  $E(\theta)$ , Poisson's ratio  $v(\theta)$  and negative Poisson's ratio of (a)  $\text{N}_2\text{Se}_3$  (b)  $\text{P}_2\text{Se}_3$  (c)  $\text{As}_2\text{S}_3$  (d)  $\text{Se}_3\text{As}_2$ .

Table S2 Extremes of the in-plane Young's modulus and Poisson's ratio for  $X_3M_2$  ( $X=S, Se$ ;  $M=N, P, As$ )

Formula	Young's Modulus				Poisson's Ratio			
	Maximum		Minimum		Maximum		Minimum	
	$E$ (GPa)	$\theta$ ( $^{\circ}$ )	$E$ (GPa)	$\theta$ ( $^{\circ}$ )	$\nu$	$\theta$ ( $^{\circ}$ )	$\nu$	$\theta$ ( $^{\circ}$ )
$S_3N_2$	82.26	45	26.38	90	0.7405	0	<b>-0.0259</b>	45
$Se_3N_2$	84.92	18	32.59	90	0.4182	0	<b>-0.0468</b>	44
$S_3P_2$	63.60	17	17.07	90	0.8229	0	0.0157	45
$Se_3P_2$	56.67	23	9.74	90	1.1553	0	<b>-0.1999</b>	42
$S_3As_2$	48.14	26	10.97	90	0.8229	0	<b>-0.0836</b>	44
$Se_3As_2$	56.46	22	10.24	90	1.0799	0	<b>-0.1857</b>	42

### Equation S1

Variables defined with elastic constants  $C_{ij}$  for calculating orientation-dependent in-plane Young's modulus  $E(\theta)$  and Poisson's ratio  $\nu(\theta)$ .

$$\nu_{ZZ} = \frac{C_{12}}{C_{22}}$$

$$d_1 = \frac{C_{11}}{C_{22}} + 1 - \frac{C_{11}C_{22} - C_{12}^2}{C_{22}C_{66}}$$

$$d_2 = -(2\frac{C_{12}}{C_{22}} - \frac{C_{11}C_{22} - C_{12}^2}{C_{22}C_{66}})$$

$$d_3 = \frac{C_{11}}{C_{22}}$$

$$Y_{ZZ} = \frac{C_{11}C_{22} - C_{12}^2}{C_{22}}$$

### Reference

1. Y. Du, J. Maassen, W. Wu, Z. Luo, X. Xu and P. D. Ye, *Nano Letters*, 2016, **16**, 6701-6708.
2. J. Han, J. Xie, Z. Zhang, D. Yang, M. Si and D. Xue, *Applied Physics Express*, 2015, **8**, 041801.